

Article

Morphology Modulation in Self-Assembly of Chiral 2-Hydroxy-2-Phenylacetic Acids in Polymeric Diluents

Baiq Firyal Salsabila Safitri and Eamor M. Woo * 

Department of Chemical Engineering, National Cheng Kung University, No. 1, University Road, Tainan 70101, Taiwan; n36097079@gs.ncku.edu.tw

* Correspondence: emwoo@mail.ncku.edu.tw; Tel.: +886-6-275-7575 (ext. 62670)

Abstract: This study focused on the chirality effects that control the lamellar bending sense in self-assembled crystals of chiral 2-hydroxy-2-phenylacetic acids. 2-Hydroxy-2-phenylacetic acid or mandelic acid (MA) was crystallized in the presence of poly(4-vinyl phenol) (PVPh), and its crystalline structures and morphologies were assessed using polarized optical microscopy (POM) and scanning electron microscopy (SEM). MA of two opposite chiral forms (S- and R-) was crystallized with PVPh as the morphology modulator; with adjustment of the PVPh content, the morphology of MA crystals transforms from ring-banded spherulites to highly dendritic spherulites. For MA/PVPh (50/50 wt./wt.) blend and neat MA at same T_c , the dendritic spherulites are packed with single crystals where the lamellae bend at a specific direction varying with T_c and chirality. Contrary to conventional thought, the bending senses of the MA lamellae in the dendritic spherulites are not solely governed by the MA molecular chirality (S or R), but also by T_c . Only at high T_c (>65 °C) is the lamellar bending direction in dendritic spherulites of (S)-MA or (R)-MA blended with PVPh dictated by the chirality, i.e., displaying counterclockwise and clockwise bending direction for (S)-MA/PVPh and (R)-MA/PVPh, respectively. Nevertheless, at low T_c (45 °C), the bending sense of dendritic spherulites displays an opposite direction from those at the higher T_c , which is to say that the chirality alone does not control the lamellar bending direction.

Keywords: 2-hydroxy-2-phenylacetic acids; bending sense; chirality; lamellae assembly



Citation: Safitri, B.F.S.; Woo, E.M. Morphology Modulation in Self-Assembly of Chiral 2-Hydroxy-2-Phenylacetic Acids in Polymeric Diluents. *Crystals* **2022**, *12*, 807. <https://doi.org/10.3390/cryst12060807>

Academic Editor: Jean-Marc Haudin

Received: 16 May 2022

Accepted: 3 June 2022

Published: 7 June 2022

Publisher's Note: MDPI stays neutral with regard to jurisdictional claims in published maps and institutional affiliations.



Copyright: © 2022 by the authors. Licensee MDPI, Basel, Switzerland. This article is an open access article distributed under the terms and conditions of the Creative Commons Attribution (CC BY) license (<https://creativecommons.org/licenses/by/4.0/>).

1. Introduction

Chirality is a fascinating phenomenon in nature that has been observed in organic and inorganic materials: small molecules [1–5], polymers [6–13], and more complex biological systems [14,15]. In 2007, Oaki and Imai [16] demonstrated that D- and L-aspartic acid (D-Asp and L-Asp) exhibited helical morphologies following water evaporation in an agar matrix (which acts as a modulating agent). D-Asp and L-Asp are two optically isomeric forms of bioorganic aspartic acid (Asp) with identical physical properties. Additionally, with the aid of an agar matrix, the helical crystalline architecture's handedness was controlled by the chirality of Asp molecules: left- and right-handed twist from D- and L-Asp, respectively. In 2014, Wang and Prud'homme [11] combined nonequimolar poly(D-lactide) (PDLA) and poly(L-lactide) (PLLA). After mixing, mutual isomers form PLA complexes (scPLA). An excess of PDLA or PLLA resulted in the flat-on branches bending counterclockwise and clockwise, respectively. However, the rotation direction was reversed when the film thickness increased. PLLA-rich films deflected clockwise, while PDLA-rich films deflected counterclockwise. Maillard and Prud'homme [9] also observed a blend of PDLA or PLLA with poly(ethylene glycol) (PEG) at composition 75/25 with sample thickness 10 nm. PDLA/PEG (75/25) and PLLA/PEG (75/25) have star-shaped crystal structures composed of edge-on lamellae radiating out from a central point with counterclockwise and clockwise bending directions, respectively. These bending directions are in opposition to PLA's chirality. In addition, they reported that dendritic crystals in

the trigonal shape of PLLA/PDLA blend with a sample thickness of 20 nm crystallizes in counterclockwise- and clockwise-circularly bending sense for PDLA/PLLA (75/25) and PDLA/PLLA (25/75) blends, respectively. This result is consistent with the chirality of PLA; when PLLA is in excess, the bending direction is counterclockwise and when PDLA is in excess, the bending direction is in the opposite direction [10]. Though considerable effort has been expended on the subject, it remains a mystery how the chiral sense develops on crystallization morphology.

The crystallization morphology is determined by the proximity of the equilibrium state (i.e., the driving force for crystallization) and the growth condition [2,17,18], such as temperature [19], the composition of diluents, preparation procedures [20], and tacticity or chirality [9–11,21–23]. On the other hand, in the case of a chiral compound, other important factors also play a role in the lamellar bending sense, such as film thickness [12,24,25] and blend composition [9]. Poly(*p*-vinyl phenol) (PVPh) has been reported to have a high degree of interaction with some semicrystalline polymers and further possesses the ability to form dendritic patterns [26,27]. With increasing content of PVPh, poly(ethylene oxide) (PEO) gradually transforms from regular Maltese-cross spherulites into dendritic spherulites showing no Maltese-cross optical extinction. The intermolecular hydrogen bonding of PVPh with PEO results in the formation of a variety of morphologies and reduces the tendency of PEO crystallization [26]. 2-Hydroxy-2-phenylacetic acid or mandelic acid (MA) is a chiral molecule with R and S enantiomeric forms. MA has been reported to exhibit a variety of morphologies as a result of evaporation-induced crystallization from MA solutions, which is dependent on the evaporation conditions, including the solvent type and evaporation temperature [28,29]. At medium evaporation rates, MA forms fractal-like dendritic morphology when crystallized at 35 °C [28].

In this article, we blended MA with amorphous PVPh and crystallized it under different evaporation temperatures to induce diversified lamellar-bending morphology. The effect of chirality and evaporation temperature was examined to clarify the relation of the corresponding morphology. Eventually, correlation between the bending sense of the MA spherulite can be established via careful inspection of the crystal assembly of the diversified MA crystals.

2. Materials and Methods

2-Hydroxy-2-phenylacetic acid or mandelic acid (MA) with molecular weight (MW) = 152.15 g/mol, $T_m = 131$ °C was obtained from Sigma-Aldrich (St. Louis, MO, USA). Poly(4-vinyl phenol) was purchased from Polyscience (City of Brotherly Love, PA, USA), with molecular weight (MW) = 22,000 g/mol, and $T_g = 150.5$ °C. A binary mixture of different compositions of (S)-MA/PVPh or (R)-MA/PVPh was prepared by dissolving in *p*-dioxane with the concentration of 4 wt.%. A drop of solution was cast into a microglass slide at various crystallization temperatures, and the solvent was allowed to evaporate completely. Specimens were left on a hot stage at specified isothermal temperatures until they crystallized completely.

2.1. Apparatus

2.1.1. Polarized-Light Optical Microscopy (POM and OM)

A polarized-light optical microscope (POM) was equipped with an automatic exposure device (Nikon NFX-DX, Nikon Corp., Tokyo, Japan), a heating stage (Linkam THMS-600, Linkam Scientific Instrument Ltd., Surrey, UK), a temperature control device (Linkam T95, Linkam Scientific Instrument Ltd., Surrey, UK), and a digital image capture system (Nikon Digital Sight DS-U1). The samples were crystallized at different isothermal temperatures by solvent evaporation, and the fully grown MA spherulites were observed. The samples were observed using 4×, 10×, and 40× objective lenses with calibrated image scales.

2.1.2. High-Resolution Field-Emission Scanning Electron Microscopy (HR-FESEM)

Scanning electron microscopy (Hitachi SU8010) was used for characterizing the top surfaces of samples in better resolution and greater magnifications than results from POM. Prior to SEM observation, samples were coated with platinum using vacuum sputtering (10 mA, 300 s) and observed under 1 kV at an 8 mm working distance.

3. Results and Discussion

3.1. Effect of Chirality on Assembly Morphology

Mandelic acid (MA) films can form dendrites upon dilution with other polymers such as PVPh via evaporation-induced crystallization. MA/PVPh blend systems at different wt. ratios exist as dendritic spherulites, but the morphology is different, as shown in Figure 1A,B. MA morphological pattern variation can be obtained in the MA/PVPh blends of various compositions at 60 °C. Obviously, the bending sense of the lamellae in the dendritic spherulite MA varies with respect to the specific composition and crystallization temperature.

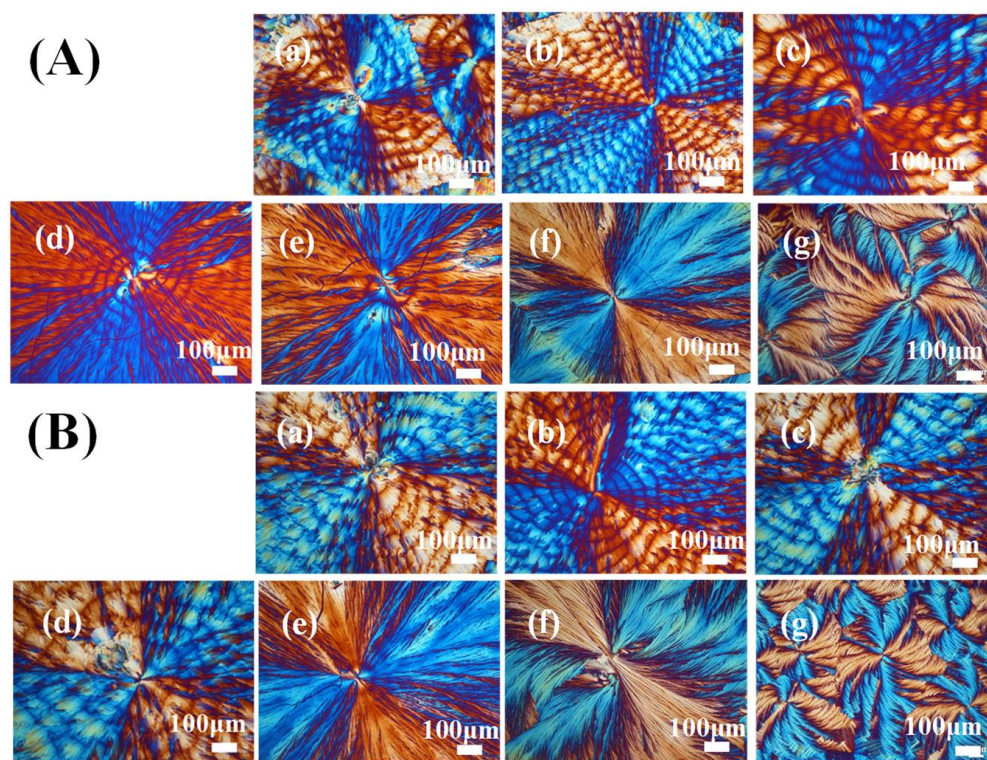


Figure 1. POM graphs of (A) (R)-MA/PVPh and (B) (S)-MA/PVPh blends crystallized at $T_c = 60$ °C for different compositions: (a) 90/10, (b) 85/15, (c) 80/20, (d) 75/25, (e) 70/30, (f) 60/40, and (g) 50/50.

When the content of amorphous PVPh is less than 20 wt.%, MA exists as ring-banded spherulites. As the content of PVPh increases, the size of spherulites decreases and the crystallization rate also drops significantly. The MA spherulites exhibit spiral bands with PVPh contents of 10–20 wt.% (with clockwise or counterclockwise spiral rotation). The spiral band exists in the center but gradually vanishes at the periphery of spherulites with increased PVPh content to 25–30 wt.% in MA/PVPh blends. At 40 wt.% of PVPh content, MA exhibits dendritic spherulites with straight dendrites. Finally, with 50 wt.% content the (R)-MA and (S)-MA forms fully dendritic spherulites with side branches curving in the clockwise and counterclockwise directions, respectively. Therefore, MA/PVPh (50/50) is used for an in-depth analysis.

3.2. Lamellar Bending in Dendritic Spherulites

In 2014, Wang and Prud'homme [11] observed dendritic spherulite morphology of PLLA/PDLA at various compositions and crystallization temperatures. The morphologies exist as dendritic spherulites that have different curvature. The curvature of the spherulites is determined by the film thickness, the chirality of the excess enantiomer, and the crystallization temperature. Furthermore, evaporation parameters, predominantly temperature, have been shown to significantly affect crystallization kinetics and the final morphology of the crystals [21]. The crystal morphology is all dendritic spherulites, as shown in Figures 2 and 3. At lower T_c (30–35 °C), (R)-MA (Figure 2a), and (S)-MA (Figure 3a) crystals grow with straight dendrites. Nevertheless, (R)-MA (Figure 2i–k) and (S)-MA (Figure 3i–k) crystals grow into fibrous dendritic spherulites with curved dendrites at higher T_c (60–65 °C). However, the (R)-MA and (S)-MA crystal curvatures are opposite to each other: (R)-MA shows clockwise dendrites and (S)-MA shows counterclockwise dendrites. Moreover, the dendrites become less compact with increasing evaporation temperature. A novel bending of fibrous dendrite spherulites exists at the intermediate T_c (36–48 °C). Interestingly, the bending curvatures in MA at intermediate temperatures are opposite to the MA dendrites at higher temperatures.

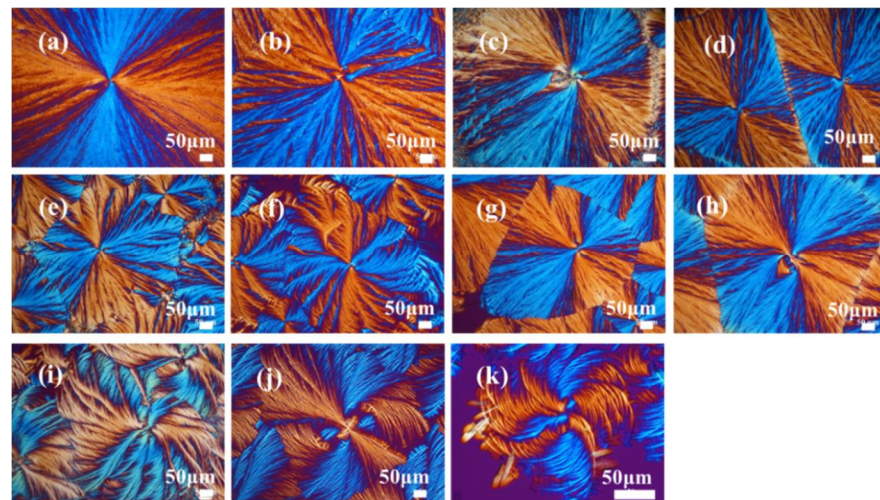


Figure 2. POM graphs of (R)-MA/PVPh (50/50) blend at different T_c : (a) 30, (b) 35, (c) 36, (d) 40, (e) 45, (f) 48, (g) 50, (h) 55, (i) 60, (j) 63, and (k) 65 °C.

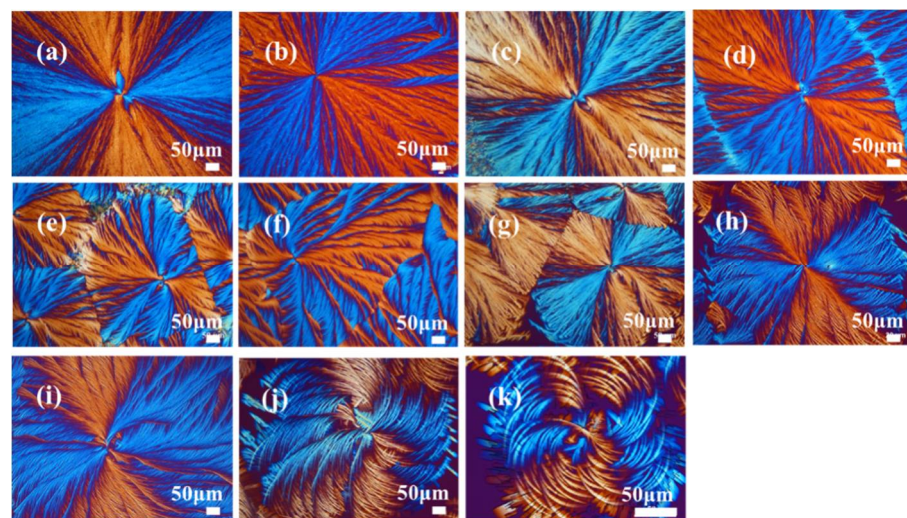


Figure 3. POM graphs of (S)-MA/PVPh (50/50) blend at different T_c : (a) 30, (b) 35, (c) 36, (d) 40, (e) 45, (f) 48, (g) 50, (h) 55, (i) 60, (j) 63, and (k) 65 °C.

To appreciate the time-evolution of the dendritic MA morphology from nucleation to completion, an example of in situ monitoring is demonstrated in Figure 4. One sees that the bending the bending starts at early stages with a lesser scale, but the bending becomes more obvious in later stages toward completion.

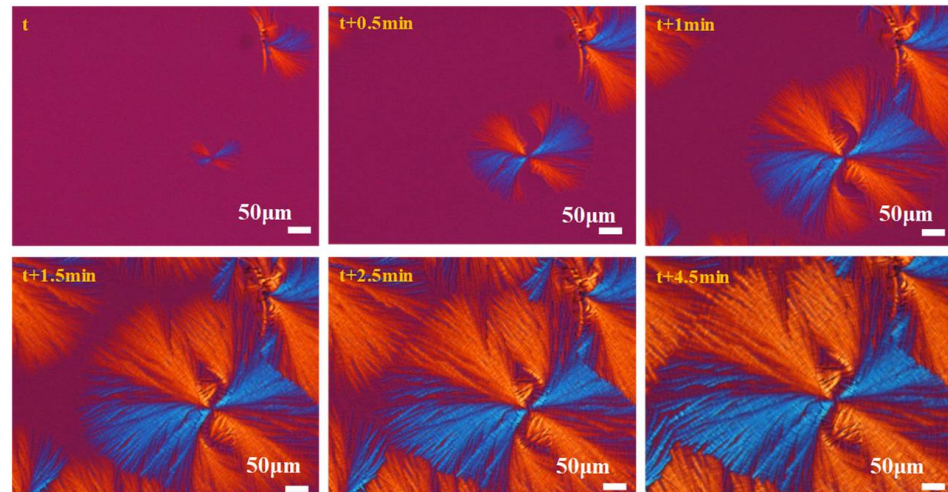


Figure 4. In situ evolution of MA morphology (from R-MA/PVPh (50/50)) upon solvent-evaporation crystallization at 60 °C, from t to t + 4.5 min, where t = initiation of first trace of nuclei.

In 2016, Woo et al. [12] reported a similar phenomenon in chiral poly(lactic acid) (PLA) by altering the T_c . Singfield et al. [7] demonstrated in 1995 that polyepichlorohydrin exhibits clockwise (R-form) or counterclockwise (S-form) bending of what they termed “pinwheel-like” dendrites; however, the straight dendrites appear in a racemic blend of polyepichlorohydrin. They stated that the chirality of the polymer chains imposes significant constraints on the lamellar organization in two chiral forms of polyepichlorohydrin (R and S chirality).

Both rotation of the axis of Maltese-cross and bending sense of the lamellae packed in the dendritic MA spherulites appear to depend on the temperature of crystallization. Rotation of the Maltese-cross is depicted in the schematics for the POM birefringent morphology in (R)-MA/PVPh and (S)-MA/PVPh, as shown in Figure 5a,b. Intriguingly, the Maltese-cross rotates in just the opposite direction of the bending sense of lamellae in the spherulites. Bending sense of lamellae appears to be opposite to that of the axis-rotation direction. With an increase in T_c , the Maltese-cross rotates in the clockwise direction; oppositely, the lamellae in the dendritic spherulites bend in the counterclockwise direction and vice versa. The schemes show that the chirality of MA induces exactly opposite rotation and lamellae bending sense when crystallized at the same T_c .

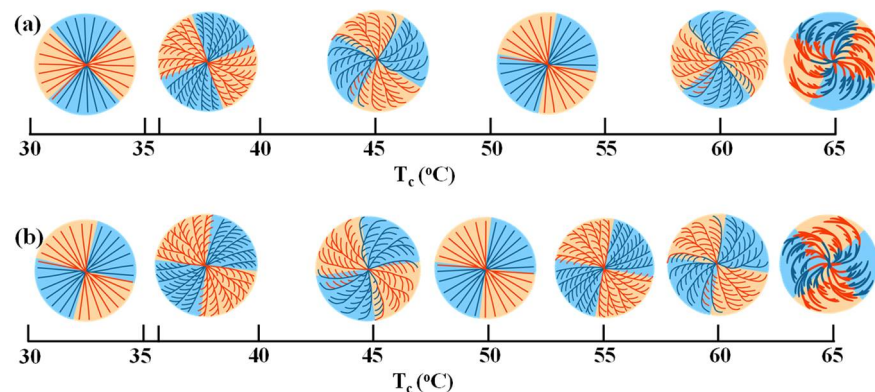


Figure 5. Schematics for the birefringent patterns of (a) (R)-MA/PVPh (50/50) and (b) (S)-MA/PVPh (50/50) blend at different crystallization temperatures.

Apart from that, various thicknesses of samples were used to clarify the bending sense on the MA crystalline morphology. We can conclude from Figure 6a,b that bending in dendritic spherulites does not change with increasing sample thickness. According to the POM results discussed above, the bending sense of MA spherulites can display three different trends. These three categories are (i) straight dendrites, (ii) bend in line with chirality, and (iii) bend opposite to chirality, which means that molecular chirality of MA does not govern all aspects of crystallization. Therefore, the bending sense of spherulites cannot be easily predicted as other essential factors also play a role, such as crystallization temperature. MA/PVPh (50/50) at a crystallization temperature of 45 and 65 °C have the clearest morphology, so these temperatures were chosen for an in-depth future discussion.

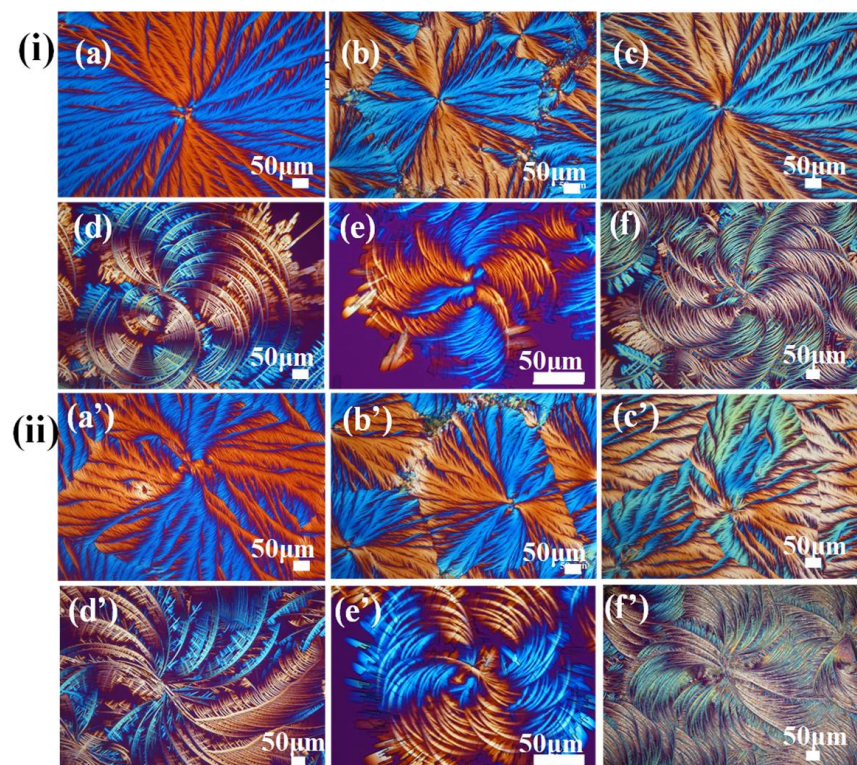


Figure 6. POM graphs of (i) (R)-MA/PVPh (50/50) and (ii) (S)-MA/PVPh (50/50) blends crystallized at (a–c, a'–c') $T_c = 45$ °C and (d–f, d'–f') $T_c = 65$ °C. The film thickness is (a,d) 2–5; (b,e) 10–20; and (c,f) 25–30 μm .

3.3. Crystalline Morphology and Crystal Arrangement of Bending Dendritic Spherulites

According to previous POM results, the (R)-MA/PVPh and (S)-MA/PVPh systems exhibit varying dendritic spherulite bending. Follow-up experiments were conducted using an equimolar ratio (50/50) and crystallization conditions ($T_c = 45$ and 65 °C), and SEM discussed the lamellae growth in detail. The comparison of POM and SEM images of (R)-MA/PVPh (50/50) blend at $T_c = 45$ °C, as shown in Figure 7a, depicts the entire spherulites, with Figure 7b zooming to the nucleus center. The initial crystallization stage of the (R)-MA/PVPh (50/50) blend results in sheaf-like nuclei. When the crystallization time increases, the sheaf-like nuclei evolve into dendritic spherulites with a curvature or lamellar bending. Figure 7b depicts the nucleus's lamellae bending to evolve from nuclei. As it grows, it is bent in a tangential direction and fans out in a counterclockwise direction, predominantly with multiple branches, to fill the (R)-MA spherulite. A unique feature is observed in the lamellae bending near the nucleus of (R)-MA spherulites, where a portion of the nucleus sheaves are spawned from straight bundles in perpendicular direction but bent in counterclockwise sense toward the tangential direction, while the straight sheaves grow radially before bending in counterclockwise sense to merge into the same tangential direction.

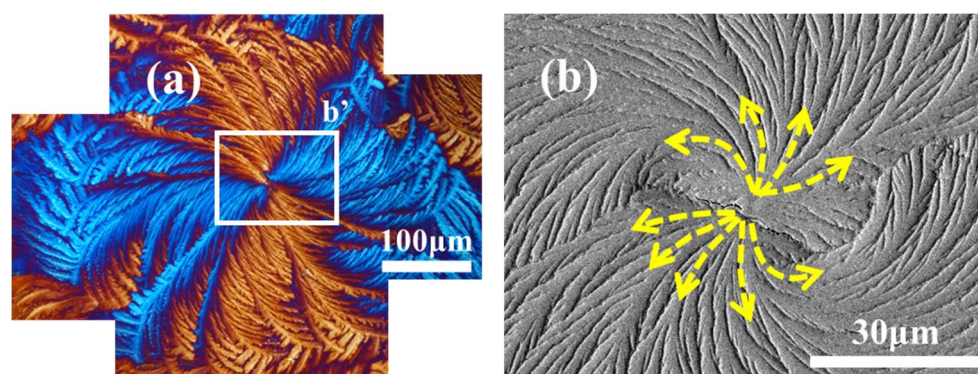


Figure 7. (a) POM, b' indicating the white-squared region to be zoomed-in by SEM and (b) SEM micrograph of (R)-MA/PVPh (50/50) blend crystallized at 45 °C.

Obviously, the nucleus geometry governs the crystal growth in R- and S-MA. For polymers, it is known that the initial geometry of the nucleus sheaf crystals may strongly govern the patterns of subsequent crystal growth into final aggregated spherulites [30,31]. For poly(L-lactic acid) (PLLA) spherulites, Yeh and Woo [30] conducted delicate fracturing across the thickness sections to expose the interior lamellae assembly, and discovered there are three types of spherulites: (1) circularly ringed (Type 1), (2) hexagon-shaped (Type 2), and (3) circularly core-striped (Type 3), and such morphological diversification originates from three different types of initial nuclei geometries: poly(nonamethylene terephthalate) (PNT) Type-1 and Type-2, are done with detailed analyses using polarized-light optical microscopy (POM) in situ CCD recording; the periodic assembly morphologies are characterized using atomic-force microscopy (AFM) and scanning electron microscopy (SEM). Similarly, dual types of periodically ring-banded morphology in poly(nonamethylene terephthalate) (PNT) (termed as Type-1 and Type-2) have been correlated with nuclei geometry [31], where a specific type of periodically banded PNT spherulite is initiated from either highly elongated sheaf-like or well-rounded nuclei, and the nucleation geometry and crystallization parameters collectively lead to development of multiple types of banded PNT spherulites of different relative fractions.

Figure 8a shows each of the main stalks of (R)-MA exploded into closely packed side branches that grow in the counterclockwise bending rhythm. As illustrated in Figure 8a, numerous primary stalks extend from nuclei crystals and bend in unison from the start to emerge into another primary stalk. They all bend counterclockwise in unison up to the terminating peripherals. Figure 8b–d depicts the entire branch, the primary and secondary branches, and the secondary branch's edge region, respectively. The secondary branch of spherulites grows from the primary (Figure 8c), which is indicated by a yellow dashed line. Figure 8c illustrates this phenomenon, with primary and secondary branches denoted by black and yellow dashed lines, respectively. Another branch grows (red line) from secondary branches, resulting in closely packed side branches. Zoomed-in detailed lamellar arrangement of dendritic spherulites is shown in Figure 8d, which depicts that the dendritic spherulites are composed of discrete single-crystal-like flat-on lamellae.

A comparison of POM and SEM micrographs of crystallized (R)-MA/PVPh (50/50) blend crystallized at $T_c = 65$ °C is demonstrated in Figure 9a depicting the entire spherulite, while Figure 9b depicts the spherulites' center. As illustrated in Figure 9b, dendrites originate from the nucleus region, where a single strand of initially straight nuclei resembling fibers splays out spontaneously into four or more arms, all growing in clockwise-bending sense in the dendritic spherulites. Divergence is observed in the dendritic spherulites at various crystallization temperatures. At an intermediate temperature ($T_c = 45$ °C), numerous main stalks explode outward from the nucleus center. In contrast, at higher temperature ($T_c = 65$ °C), fewer main stalks grow from the nucleus center, and entire spherulites are less compact than at intermediate temperatures. This difference is due to the depression of the (R)-MA spherulite growth rate at higher temperatures.

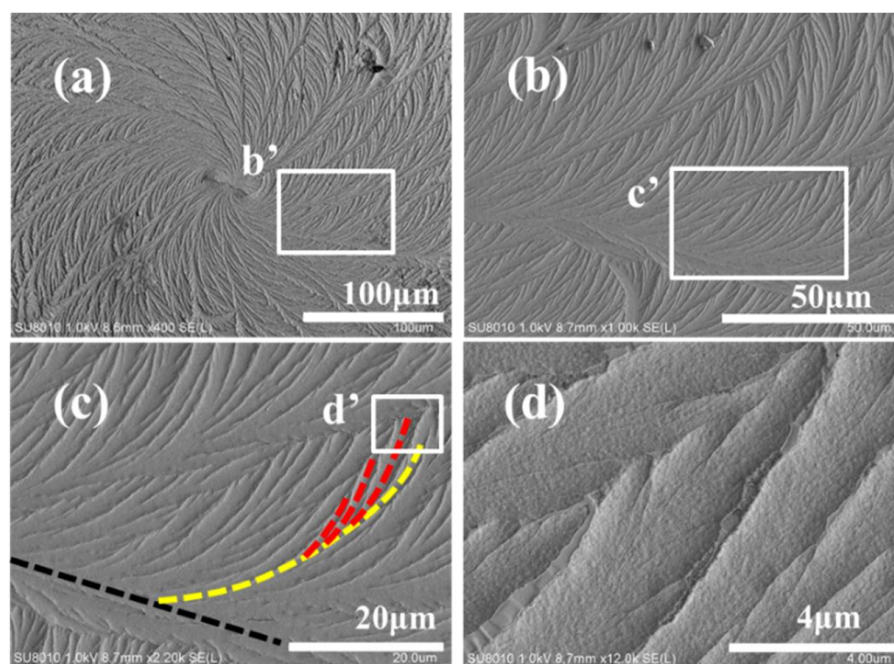


Figure 8. (a) SEM micrographs: (b–d) enlarged images of the square regions—b', c', and d' for (R)-MA/PVPh (50/50) dendritic spherulite crystallized at $T_c = 45^\circ\text{C}$.

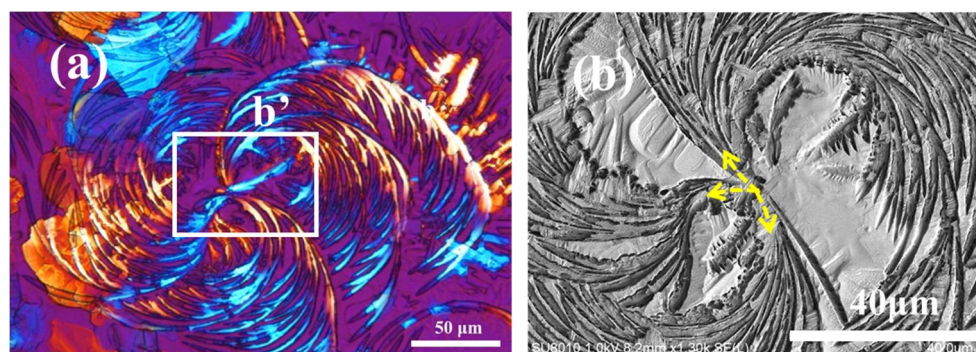


Figure 9. (a) POM, b' indicating the white-squared region to be zoomed-in by SEM and (b) SEM micrograph of (R)-MA/PVPh (50/50) blend crystallized at $T_c = 65^\circ\text{C}$.

An intriguing feature is observed in the different birefringence bands if one zooms into one single sector of the (R)-MA spherulite. The POM and SEM images in Figure 10a,b demonstrate a correlation between a single branch's three distinct types of birefringence of lamellar spots. As illustrated in Figure 10c–e, orange and blue birefringence corresponds to the periodic bending in flat-on lamellae (see scheme in lower-right). The flat-on lamellae of dendritic spherulites are organized by single crystals for orange and blue birefringence. Crystal orientation differences do not cause the alternate optical orange or blue birefringence observed in POM micrographs; instead, the periodic branching to different bending directions is responsible for the alternate optical bands.

It has been established that (R)-MA contains a chiral optical center (R-form), and the molecules of (R)-MA in crystal lattices are right-handed [32]. Lamellar bending occurs in the counterclockwise direction in the (R)-MA/PVPh (50/50) blend at $T_c = 45^\circ\text{C}$, indicating that the lamellae grow oppositely with the optical chiral center of MA. Nonetheless, the clockwise lamellar bending in the (R)-MA/PVPh (50/50) blend at $T_c = 65^\circ\text{C}$ indicates that the lamellae grow in line with the optical chiral center of MA at higher crystallization temperatures. It is quite fascinating that the bending direction of MA spherulites in the (R)-MA/PVPh (50/50) blend corresponds to their chirality, which is right-handed or clockwise at higher temperatures but reversible at lower temperatures. Furthermore,

the crystallization of the (S)-MA/PVPh (50/50) blend is observed to determine whether chirality and temperature both could dictate the bending direction. Effect of chirality on the bending sense of lamellae in crystal self-assembly was also observed in other organic compounds. As previously reported by Oaki et al. [16], chiral aspartic acid had the same structure but faced opposite directions: D-Asp was left-handed, while L-Asp was right-handed. Thus, if chirality affects the bending sense of dendritic spherulites in the (R)-MA/PVPh blend, the spherulites in the (S)-MA/PVPh blend should bend in the opposite direction as that in the (R)-MA/PVPh blend. It is worth noting that the bending is related to the chirality of MA only at higher temperatures (60–65 °C), not at intermediate temperatures (36–48 °C). This indicates that other factors, in addition to molecular chirality, might cause lamellae to bend in (R)-MA/PVPh vs. (S)-MA/PVPh. These factors are almost certainly related to crystallization temperature.

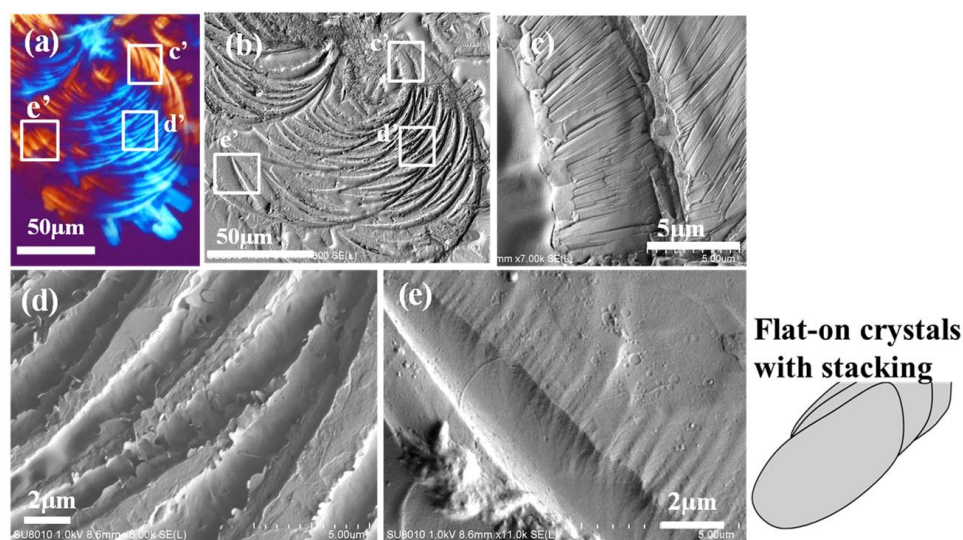


Figure 10. (a) POM graph, (b) SEM micrograph, and (c–e) zoom-in to squared regions of c', d' and e' of (b).

For comparison with the (R)-MA/PVPh system's lamellar bending behavior, the morphology of (S)-MA/PVPh was also examined. Figure 11a,b shows POM and SEM images of dendritic spherulites crystallized at $T_c = 45$ and 65 °C, respectively. It demonstrates unequivocally that this blend contains the same crystal pattern observed in (R)-MA at the same crystallization temperature. However, the dendritic spherulites in the (S)-MA/PVPh blend bend in a clockwise direction at $T_c = 45$ °C and in a counterclockwise direction at $T_c = 65$ °C. That is, the lamellae with clockwise and counterclockwise bending in (S)-MA/PVPh (50/50) are oriented in the opposite direction to those with clockwise and counterclockwise bending in (R)-MA/PVPh (50/50), as previously discussed. (R)-MA/PVPh and (S)-MA/PVPh have identical patterns, but the lamellae bend in the opposite direction of the lamellar packed in the spherulites. As illustrated in the SEM micrograph of Figure 11b, both types of spherulites begin with sheaf-like nuclei. The stalks grow in a specific bending direction as primary branches throughout the crystallization process. The final morphology in (R)-MA/PVPh and (S)-MA/PVPh appears to be identical.

The detailed lamellar structure of the (S)-MA dendritic spherulites in (S)-MA/PVPh (50/50) blend has also been observed by using SEM analysis. Figure 12a shows detailed lamellae of the (S)-MA/PVPh (50/50) blend crystallized at $T_c = 45$ °C. Figure 12b–d depicts the entire branch, the primary and secondary branches, and the secondary branch's edge region, respectively. As shown in Figure 12d, the lamellae of (S)-MA/PVPh (50/50) are composed of flat-on single crystals, which are similar to those of (R)-MA/PVPh (50/50). Nonetheless, there is a slight difference in the detailed branching patterns of the flat-on lamellae in the (S)-MA/PVPh and (R)-MA/PVPh blends. The secondary branching extends

out from the right- and left-hand-side from primary branches, where these secondary branches are indicated by yellow dashed-lines. In contrast, the secondary branches in left-hand-side stop growing when the branches impinge on other secondary branches due to competition between their growth rates.

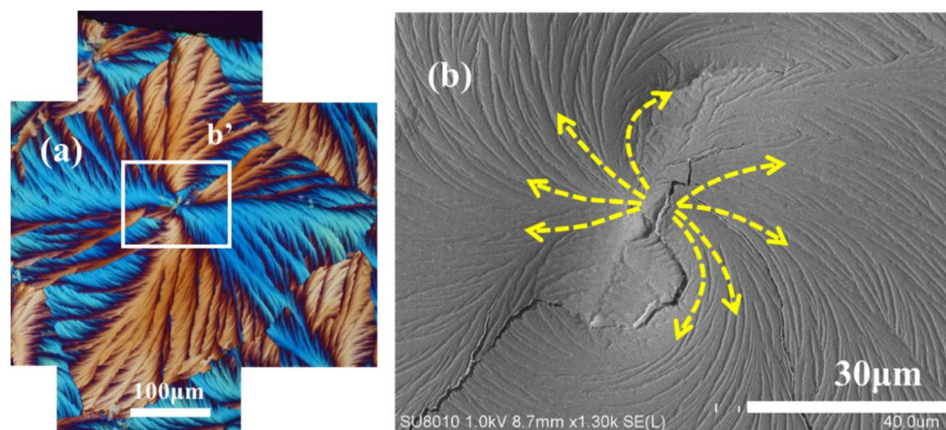


Figure 11. (a) POM, b' indicating the white-squared region to be zoomed-in by SEM and (b) SEM micrograph of (S)-MA/PVPh (50/50) blend crystallized at $T_c = 45\text{ }^\circ\text{C}$.

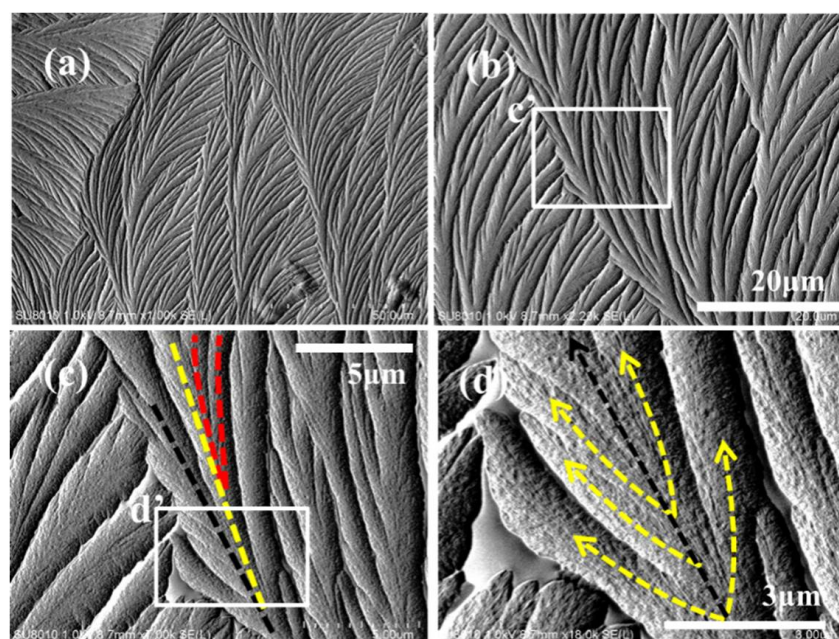


Figure 12. (a) SEM micrographs: (b–d) enlarged zoomed-in images of the squared regions—c' and d' of (S)-MA/PVPh (50/50) dendritic spherulite crystallized at $T_c = 45\text{ }^\circ\text{C}$.

The comparison of POM and SEM images of (R)-MA/PVPh (50/50) blend at $T_c = 65\text{ }^\circ\text{C}$ are demonstrated in Figure 13. Dendritic lamellae spontaneously splay out into three to four or more arms, which grow counterclockwise, as shown in Figure 13b. The POM and SEM images in Figure 13c,d demonstrate a clear correlation between two distinct types of birefringence of lamellar spots. As illustrated in Figure 13e,f, the alternate optical orange or blue birefringence bands are due to periodic branching in the tangential direction, and this assembly pattern is similar to that of the (R)-MA/PVPh (50/50). The detailed morphology indicates that lamellae of the (S)-MA/PVPh (50/50) are composed of flat-on single crystals. The direction of lamellar bending in dendritic spherulites of (R)-MA/PVPh (50/50) and (S)-MA/PVPh (50/50) at $T_c = 65\text{ }^\circ\text{C}$ appears to be determined by the chirality of the mandelic acid.

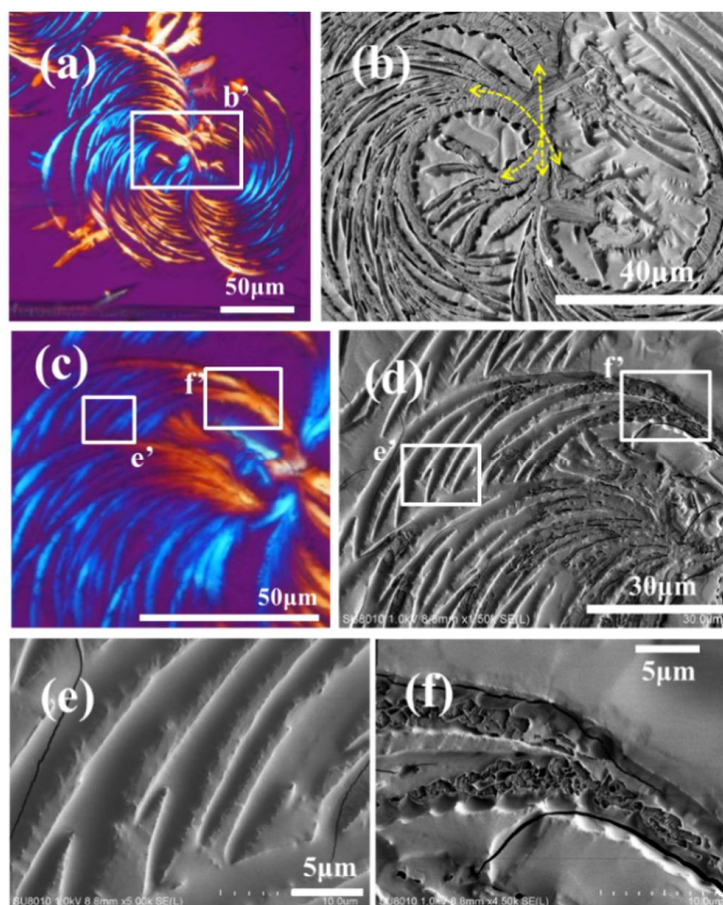


Figure 13. (a,c) POM and (b,d–f) SEM micrograph of (S)-MA/PVPh: (e,f) zoomed-in images of the squared regions— e' and f' in (c) (50/50) blend crystallized at $T_c = 65^\circ\text{C}$.

Significant findings are summarized and compared for the (R)-MA/PVPh and (S)-MA/PVPh systems where chirality- and temperature-dependent lamellar bending is observed during crystallization. However, the dendritic bending direction in (R)-MA or (S)-MA blended with PVPh is determined by the chirality of mandelic acid and the crystallization temperature. Contrary to the conventional thoughts, the dendritic spherulites in the (R)-MA/PVPh and (S)-MA/PVPh blends are predominantly characterized by flat-on lamellae, which undergo specific bending sense with respect to the kinetic factor of temperature and the thermodynamic factor of molecular chirality.

4. Conclusions

The effect of molecular chirality on the bending sense of lamellar MA crystal in MA (modulated with PVPh) can exhibit three distinct trends. These three categories are: (i) no effect with chirality ($T_c = 30\sim 35$ and 50°C), (ii) bending in line with chirality ($T_c = 60\sim 65^\circ\text{C}$), and (iii) bending opposite to chirality ($T_c = 36\sim 48^\circ\text{C}$). Both POM and SEM analyses confirm correlation of the different bending sense. From the nucleus core, sheaf-like nuclei evolve into dendritic spherulites that bend in a tangential direction and fan out predominantly with multiple branches in a counterclockwise or clockwise direction, collectively controlled by both crystallization temperature and chirality. Furthermore, all dendritic MA spherulites are packed by single-crystal-like lamellae with purely flat-on orientation without any twist, unlike many other systems showing mixed flat-on/edge-on or twist lamellae to oblique angles between these two orientations.

This work, by examining MA of two chiral forms crystallized at different values of T_c , discovered that the lamellar bending in the firewheel-like dendritic MA crystal aggregates is not fully dictated by molecular chirality. Only at high T_c ($>65^\circ\text{C}$) is the lamellar bending

direction in dendritic spherulites of (S)-MA or (R)-MA blended with PVPh dictated by the chirality, i.e., displaying counterclockwise and clockwise bending direction for (S)-MA/PVPh and (R)-MA/PVPh, respectively. Nevertheless, at low T_c (45 °C), the bending sense of dendritic spherulites display an opposite direction from those at the higher T_c , which indicates that chirality alone does not control the lamellar bending direction.

Author Contributions: The manuscript was written through contributions by both authors, who have given approval to the final version of the manuscript. B.F.S.S. conducted most of the experiments and prepared some texts in and early draft manuscript. E.M.W. conceived the original research ideas, advised/guided the experiments and analyses, and refined most of the manuscript, further structuring the texts and figures into a polished form. All authors have read and agreed to the published version of the manuscript.

Funding: This work was supported financially by a basic research grant (MOST 110-2221-E-006-004-MY2) from the Taiwan Ministry of Science and Technology (MOST), for which the authors express their gratitude.

Institutional Review Board Statement: Not applicable.

Informed Consent Statement: Not applicable.

Data Availability Statement: Not applicable.

Conflicts of Interest: The authors declare no conflict of interest.

References

1. Kovács, T.; Szücs, R.; Holló, G.; Zuba, Z.; Molnár, J.; Christenson, H.K.; Lagzi, I. Self-Assembly of Chiral Menthol Molecules from a Liquid Film into Ring-Banded Spherulites. *Cryst. Growth Des.* **2019**, *19*, 4063–4069. [[CrossRef](#)]
2. Imai, H.; Oaki, Y. Emergence of helical morphologies with crystals: Twisted growth under diffusion-limited conditions and chirality control with molecular recognition. *CrystEngComm* **2010**, *12*, 1679–1687. [[CrossRef](#)]
3. Wei, K.T.; Ward, D.L. α -Hydroxyphenylacetic Acid: A Redetermination. *Acta Crystallogr.* **1977**, *33*, 797–800. [[CrossRef](#)]
4. Patil, A.O.; Pennington, W.T.; Paul, I.C.; Curtin, D.Y.; Dykstra, C.E. Reactions of Crystalline (R)-(-) and (S)-(+)-Mandelic Acid with Amines. Crystal Structure and Dipole Moment of (S)-Mandelic Acid. A Method of Determining Absolute Configuration of Chiral Crystals. *J. Am. Chem. Soc.* **1987**, *109*, 1529–1535. [[CrossRef](#)]
5. Zhang, Y.; Mao, S.; Ray, A.K.; Rohani, S. Nucleation and growth kinetics of (R)-mandelic acid from aqueous solution in the presence of the opposite enantiomer. *Cryst. Growth Des.* **2010**, *10*, 2879–2887. [[CrossRef](#)]
6. Saracovan, I.; Keith, H.D.; Manley, R.S.J.; Brown, G.R. Banding in spherulites of polymers having uncompensated main-chain chirality. *Macromolecules* **1999**, *32*, 8918–8922. [[CrossRef](#)]
7. Singfield, K.L.; Klass, J.M.; Brown, G.R. Optically Active Polyethers. 2. Atomic Force Microscopy of Melt-Crystallized Poly(epichlorohydrin) Enantiomers and Their Equimolar Blend. *Macromolecules* **1995**, *28*, 8006–8015. [[CrossRef](#)]
8. Singfield, K.L.; Hobbs, J.K.; Keller, A. Correlation between main chain chirality and crystal “twist” direction in polymer spherulites. *J. Cryst. Growth* **1998**, *183*, 683–689. [[CrossRef](#)]
9. Maillard, D.; Prud’homme, R.E. Crystallization of ultrathin films of polylactides: From chain chirality to lamella curvature and twisting. *Macromolecules* **2008**, *41*, 1705–1712. [[CrossRef](#)]
10. Maillard, D.; Prud’homme, R.E. Differences between crystals obtained in PLLA-rich or PDLA-rich stereocomplex mixtures. *Macromolecules* **2010**, *43*, 4006–4010. [[CrossRef](#)]
11. Wang, X.; Prud’homme, R.E. Dendritic Crystallization of Poly(L-lactide)/poly(D-lactide) Stereocomplexes in Ultrathin Films. *Macromolecules* **2014**, *47*, 668–676. [[CrossRef](#)]
12. Woo, E.M.; Lugito, G.; Tsai, J.-H.; Müller, A.J. Hierarchically diminishing chirality effects on lamellar assembly in spherulites comprising chiral polymers. *Macromolecules* **2016**, *49*, 2698–2708. [[CrossRef](#)]
13. Ye, H.M.; Xu, J.; Guo, B.H.; Iwata, T. Left- or right-handed lamellar twists in poly[(R)-3-hydroxyvalerate] banded spherulite: Dependence on growth axis. *Macromolecules* **2009**, *42*, 694–701. [[CrossRef](#)]
14. Fujiki, M. Helix magic. Thermo-driven chiroptical switching and screw-sense inversion of flexible rod helical polysilylenes. *J. Am. Chem. Soc.* **2000**, *122*, 3336–3343. [[CrossRef](#)]
15. Shepherd, N.E.; Hoang, H.N.; Abbenante, G.; Fairlie, D.P. Left- and right-handed α -helical turns in homo- and hetero-chiral helical scaffolds. *J. Am. Chem. Soc.* **2009**, *131*, 15877–15886. [[CrossRef](#)]
16. Oaki, Y.; Imai, H. Stereospecific morphogenesis of aspartic acid helical crystals through molecular recognition. *Langmuir* **2007**, *23*, 5466–5470. [[CrossRef](#)]
17. Imai, H. Self-Organized Formation of Hierarchical Structures. In *Biomimneralization I*; Naka, K., Ed.; Springer: Berlin/Heidelberg, Germany, 2006; Volume 270.

18. Oaki, Y.; Imai, H. Experimental Demonstration for the Morphological Evolution of Crystals Grown in Gel Media. *Cryst. Growth Des.* **2003**, *3*, 711–716. [[CrossRef](#)]
19. Chen, T.Y.; Woo, E.M.; Nagarajan, S. Crystal Aggregation into Periodically grating-banded Assemblies in Phthalic Acid Modulated by Molten poly(ethylene oxide). *CrystEngComm* **2020**, *22*, 467. [[CrossRef](#)]
20. Shtukenberg, A.G.; Punin, Y.O.; Gunn, E.; Kahr, B. Spherulites. *Chem. Rev.* **2012**, *112*, 1805–1838. [[CrossRef](#)]
21. Chen, T.; Woo, E.M.; Nagarajan, S. Periodic Fractal-Growth Branching to Nano-Structured Grating Aggregation in Phthalic Acid. *Sci. Rep.* **2020**, *10*, 4062. [[CrossRef](#)]
22. Maillard, D.; Prud'homme, R.E. Chirality Information Transfer in Polylactides: From Main-Chain Chirality to Lamella Curvature. *Macromolecules* **2006**, *39*, 4272–4275. [[CrossRef](#)]
23. Nurkhamidah, S.; Woo, E.M. Oppositely synchronized lamellar bending in poly(L-lactic acid) versus poly(D-lactic acid) blended with poly(1,4-butylene adipate). *Macromol. Chem. Phys.* **2014**, *215*, 978–987. [[CrossRef](#)]
24. Yen, K.C.; Woo, E.M. Formation of dendrite crystals in poly(ethylene oxide) interacting with bioresourceful tannin. *Polym. Bull.* **2009**, *62*, 225–235. [[CrossRef](#)]
25. Nurkhamidah, S.; Woo, E.M. Unconventional Non-birefringent or Birefringent Concentric Ring-Banded Spherulites in Poly(L-lactic acid) Thin Films. *Macromol. Chem. Phys.* **2013**, *214*, 673–680. [[CrossRef](#)]
26. Huang, Y.P.; Kuo, J.F.; Woo, E.M. Influence of molecular interactions on spherulite morphology in miscible poly(ethylene oxide)/epoxy network versus poly(ethylene oxide)/poly(4-vinyl phenol) blend. *Polym. Int.* **2001**, *51*, 55–61. [[CrossRef](#)]
27. Lugito, G.; Nagarajan, S.; Woo, E.M. Explosive Fibonacci-sequence growth into unusual sector-face morphology in poly(L-lactic acid) crystallized with polymeric diluents. *Sci. Rep.* **2020**, *10*, 10811. [[CrossRef](#)]
28. Das, I.; Kumar, A.; Agrawal, N.R. Non-equilibrium growth patterns of carboxylic acids crystallized on microslides. *Indian J. Chem.* **1999**, *38*, 307–310.
29. Rose, H.A.; Lilly, E. dl-Mandelic Acid. *J. Chem. Crystallogr.* **1952**, *24*, 1680–1681.
30. Yeh, Y.T.; Woo, E.M. Anatomy into interior lamellar assembly in nuclei-dependent diversified morphologies of poly(L-lactic acid). *Macromolecules* **2018**, *51*, 7722–7733. [[CrossRef](#)]
31. Woo, E.M.; Tu, C.-H.; Nagarajan, S.; Lugito, G. In-Situ Growth of Nucleus Geometry to Dual Types of Periodically Ringed Assemblies in Poly(nonamethylene terephthalate). *Crystals* **2021**, *11*, 1338. [[CrossRef](#)]
32. Zhang, S.; Harasimowicz, M.T.; de Villiers, M.M.; Yu, L. Cocrystals of Nicotinamide and (R)-Mandelic Acid in Many Ratios with Anomalous Formation Properties. *J. Am. Chem. Soc.* **2013**, *135*, 18981–18989. [[CrossRef](#)] [[PubMed](#)]